The origin of diffuse Lyα halos around LAEs

(Kusakabe+18b submitted to PASJ, announced tomorrow in ArXiv:1803.08xxx)

March 28th, Sakura CLAW

Haruka Kusakabe (Univ. of Tokyo)

K. Shimasaku, **R. Momose**, M. Ouchi,

K. Nakajima, T. Hashimoto, Y. Harikane,

J. Silverman, and P. Capak

Sakura viewing party, "Hanami"

1. bring your boxed lunch and green tea from registration desks after the morning session
2. walk to Hanami place together

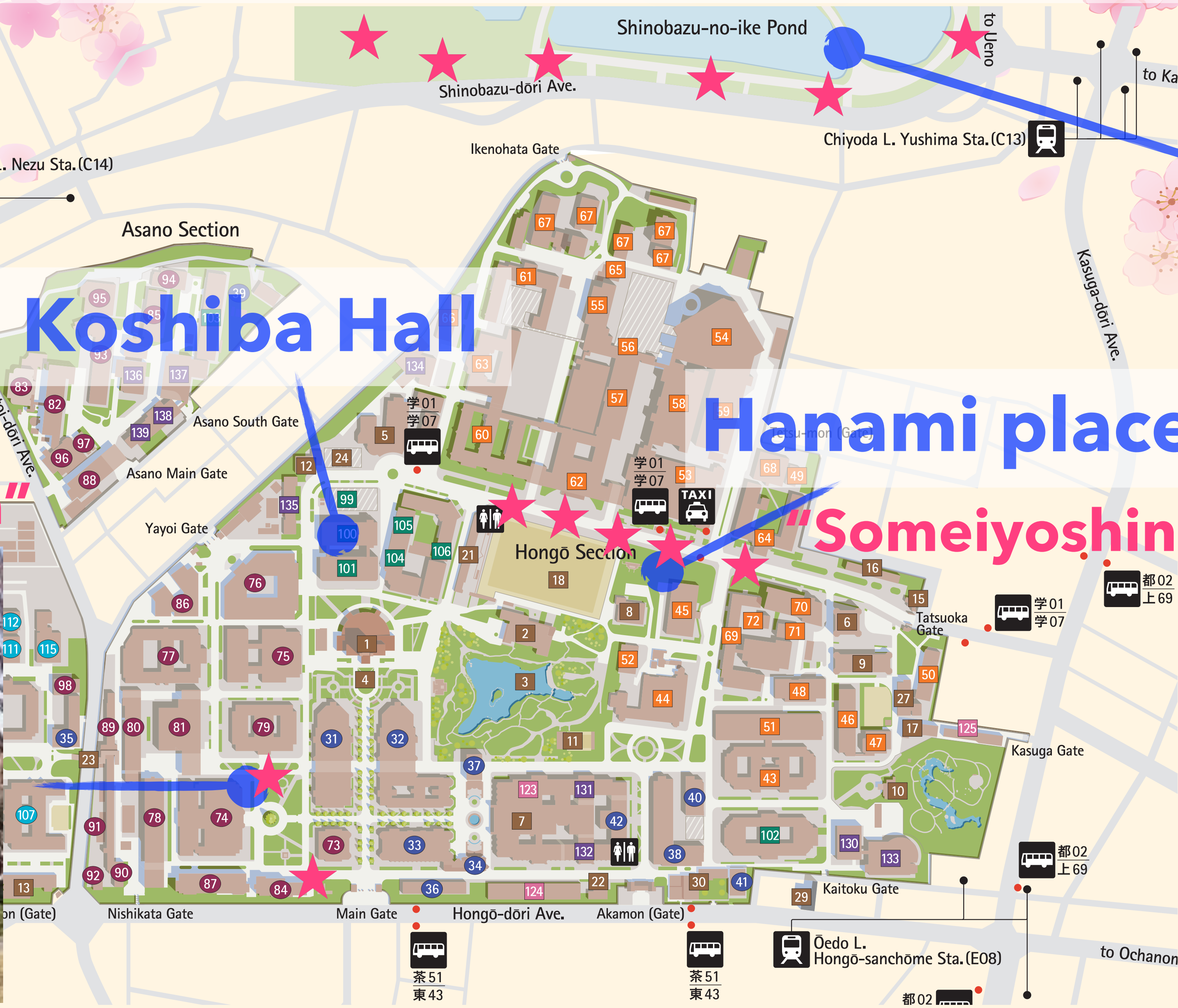

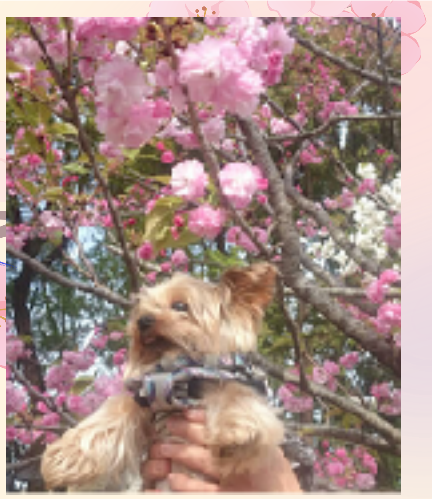

Ueno Park

The origin of diffuse Lyα halos around LAEs

(Kusakabe+18b submitted to PASJ, announced tomorrow in ArXiv:1803.08xxx)

March 28th, Sakura CLAW

Haruka Kusakabe (Univ. of Tokyo)

K. Shimasaku, **R. Momose,** M. Ouchi,

K. Nakajima, T. Hashimoto, Y. Harikane,

J. Silverman, and P. Capak

What powers Lyα halos?

(a) Cold streams (cooling radiation) **(b) Satellite Star formation** **(c) Scattered light in the CGM**

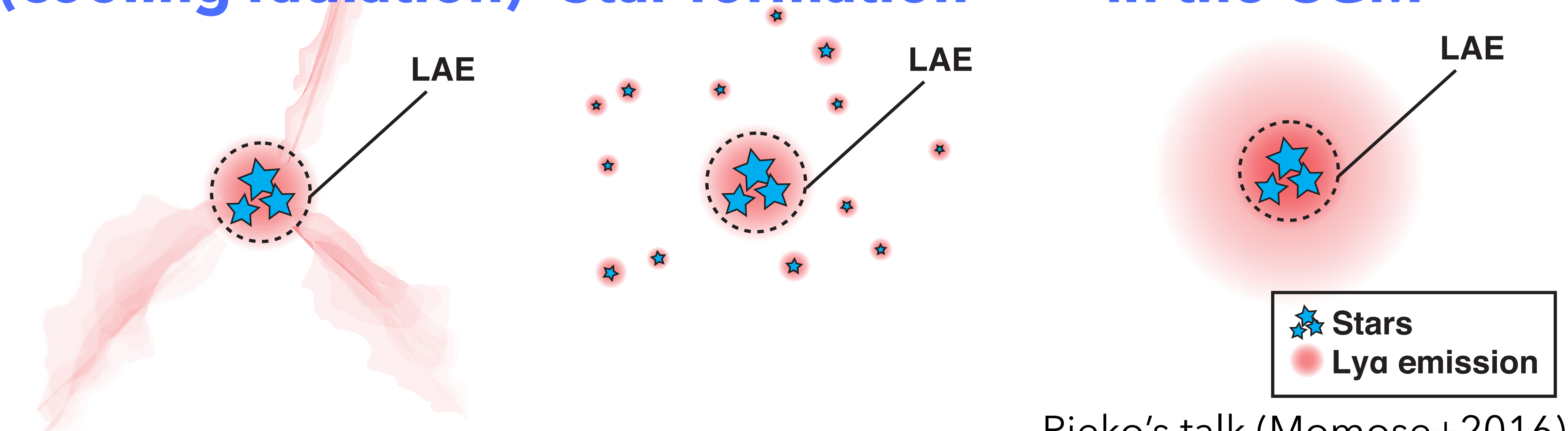

Rieko's talk (Momose+2016)

Fluorescence, shock heating by gas outflow, major merger: perhaps not important for normal SFGs

Haiman+2000; Taniguchi & Shioya 2000; Cantalupo+2005; Mori & Umemura 2006; Laursen & Sommer-Larsen 2007; Zheng+2011; Rosdahl & Blaizot 2012; Yajima+2013 Lake+2015; Mas-Ribas & Dijkstra 2016

Neither conclusive **nor** consistent previous results

(a) Cold streams (cooling radiation)

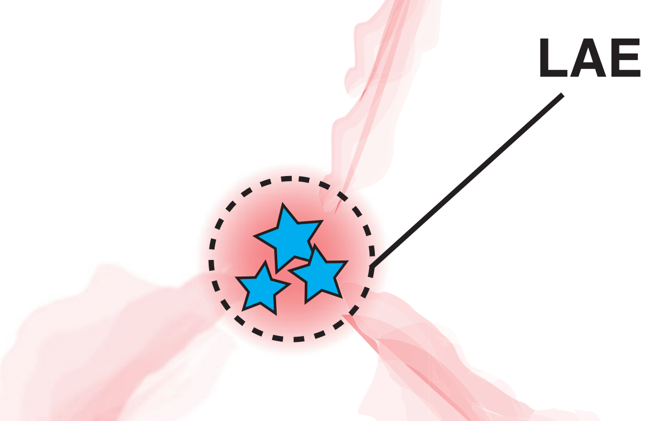

✔? Matsuda+2012
large EW

✗? Momose+2016
small EW

(b) Satellite Star formation

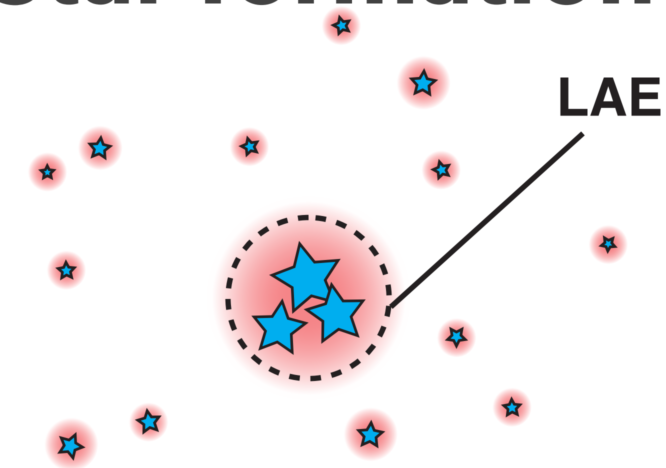

✗? Xue+2017
w/o rs - overdensity
see however MA12

✗? Leclercq+2017
w/o spatial offset

(c) Scattered light in the CGM

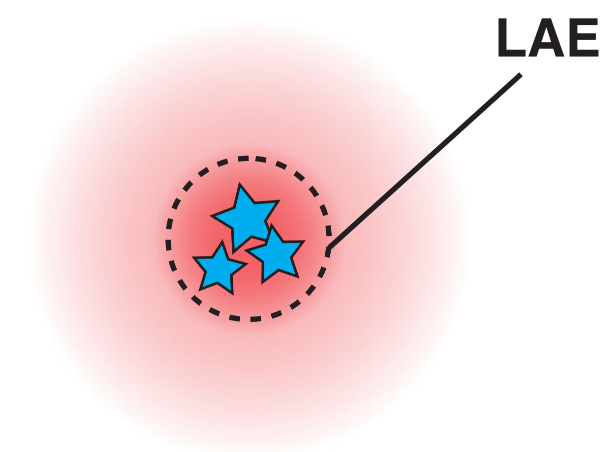

✔? Xue+2017
radial profile

✗? Lake+2015

Fluorescence, shock heating by gas outflow, major merger:
perhaps not important for normal SFGs

Rieko's talk (Momose+2016)

In this work

- Origin of LAHs from Ms (or Mh) -LAH luminosity
- Accurate estimation of Lya escape fraction, fesc(Lya)

→ Large sample of NB-LAEs with deep multi-wavelength data

Our sample & method:

~900 LAEs at z~2 in ~2000 arcmin^2 (SXDS, COSMOS)
by **Suprime-Cam** (NBtot<=25.5mag: Nakajima+2012, +2013; Konno+2016; HK+2018a)

- 10 subsamples in accordance with K, L(UV), β, L(Lya), & EW(Lya)
  →stellar mass tracers
- Mh: clustering analysis
- Ms, SFR, E(B-V): stacking + SED fitting
- LAH luminosity: stacked relation (Rieko's talk, Momose+2016)

In this work

- Origin of LAHs from **Ms (or Mh) -LAH luminosity**
- Accurate estimation of Lya escape fraction, **fesc(Lya)**

→ Large sample of NB-LAEs with deep multi-wavelength data

Our sample & method:

~900 LAEs at z~2 in ~2000 $arcmin^2$ (SXDS, COSMOS)

by **Suprime-Cam** (NBtot<=25.5mag: Nakajima+2012, +2013; Konno+2016; HK+2018a)

- 10 subsamples in accordance with **K, L(UV), β, L(Lya), & EW(Lya)**

  →stellar mass tracers
- Mh: clustering analysis
- Ms, SFR, E(B-V): stacking + SED fitting
- **LAH luminosity: stacked relation** (Rieko's talk, Momose+2016)

In this work

- Origin of LAHs from **Ms (or Mh) -LAH luminosity**
- Accurate estimation of Lya escape fraction, **fesc(Lya)**

→ Large sample of NB-LAEs with deep multi-wavelength data

Our sample & method:

~900 LAEs at z~2 in ~2000 ar

by **Suprime-Cam** (NBt ... +2016; HK+2018a)

- 10 subsample ...), β, L(Lya), & EW(Lya)
- Mh: clustering ... →stellar mass tracers
- Ms, SFR, E(B-V): ... SED fitting
- **LAH luminosity: s ... cked relation** (Rieko's talk, Momose+2016)

HSC survey for LAEs at z~2 is ongoing!

In this work

- Origin of LAHs from Ms (or Mh) -LAH luminosity
- Accurate estimation of Lya escape fraction, fesc(Lya)

→ Large sample of NB-LAEs with deep multi-wavelength data

Our sample & method:

~900 LAEs at z~2 in ~2000 arcmin^2 (SXDS, COSMOS)

by Suprime-Cam (NBtot<=25.5mag: Nakajima+2012, +2013; Konno+2016; HK+2018a)

- 10 subsamples in accordance with K, L(UV), β, L(Lya), & EW(Lya)

  →stellar mass tracers

- Mh: clustering analysis
- Ms, SFR, E(B-V): stacking + SED fitting
- LAH luminosity: stacked relation (Rieko's talk, Momose+2016)

Estimating $L(Ly\alpha)_H$ from $L(Ly\alpha)_C$

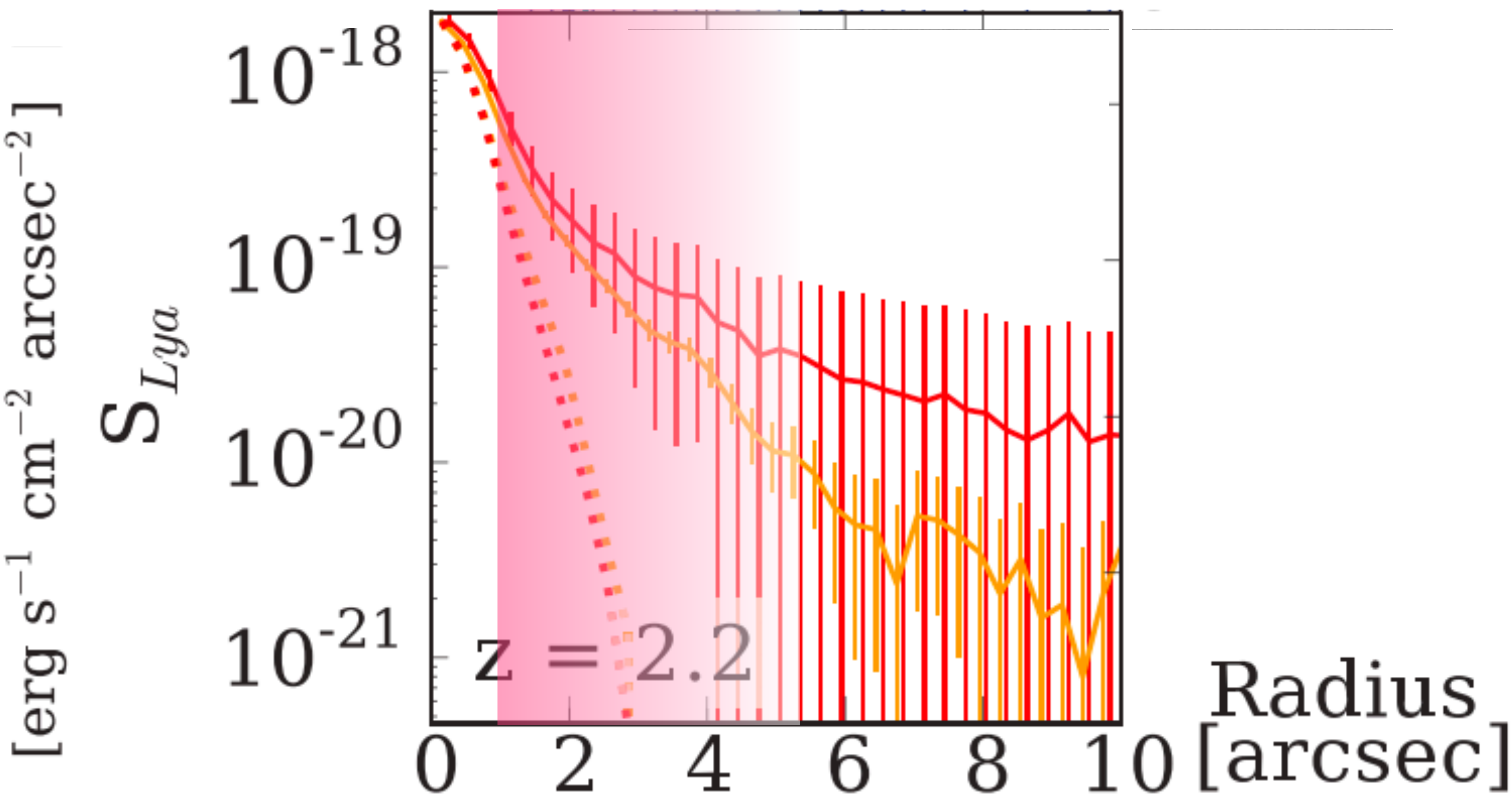

$L(Ly\alpha)_C$	$L(Ly\alpha)_H$
r<1″	r ~1″- 5″
(~8kpc)	(~8-40 kpc)

Larger scale (z=5.7, 6.6)
→Ryota's talk

Momose+2014

Estimating $L(Ly\alpha)_H$ from $L(Ly\alpha)_C$

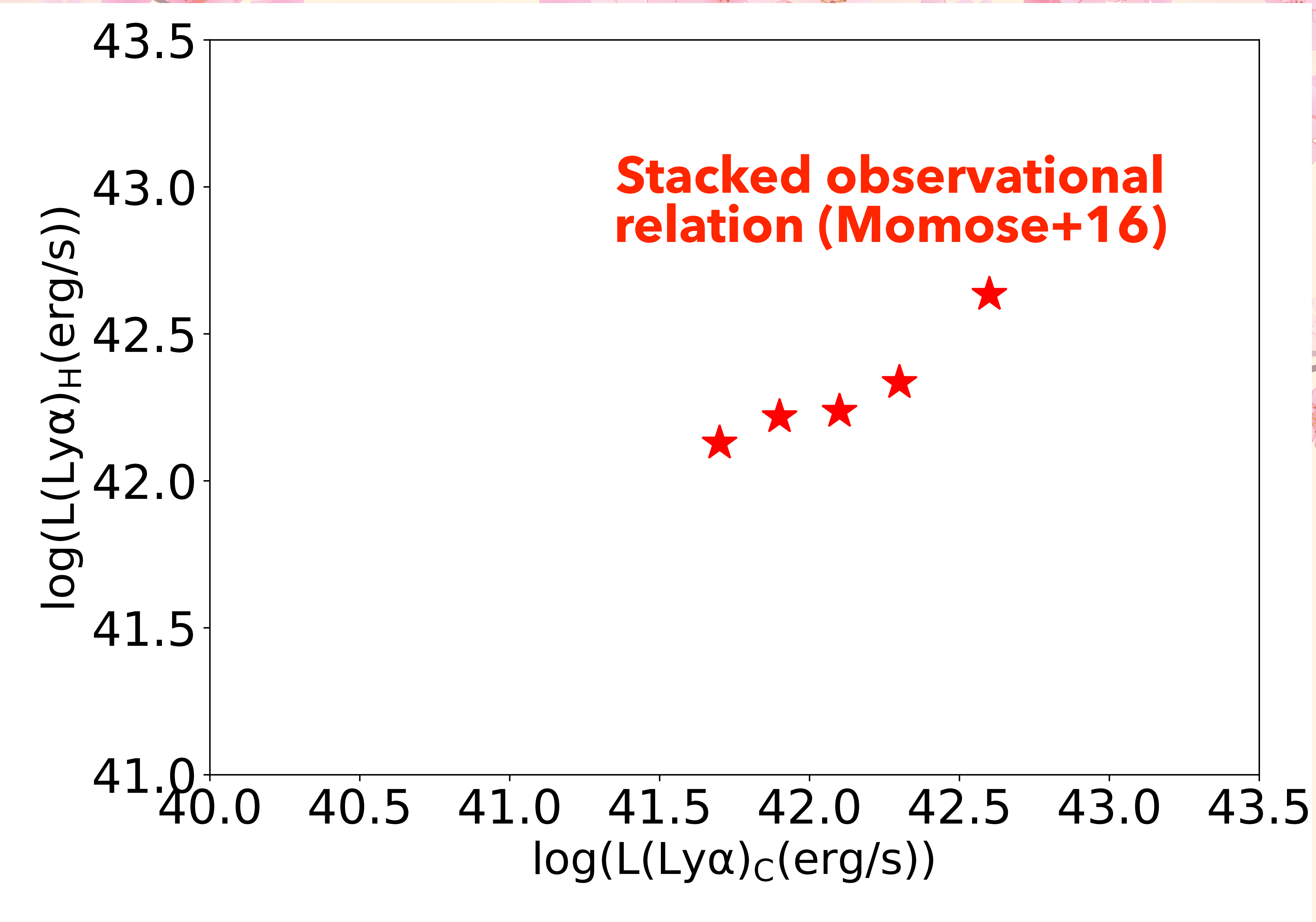

Estimating $L(Ly\alpha)_H$ from $L(Ly\alpha)_C$

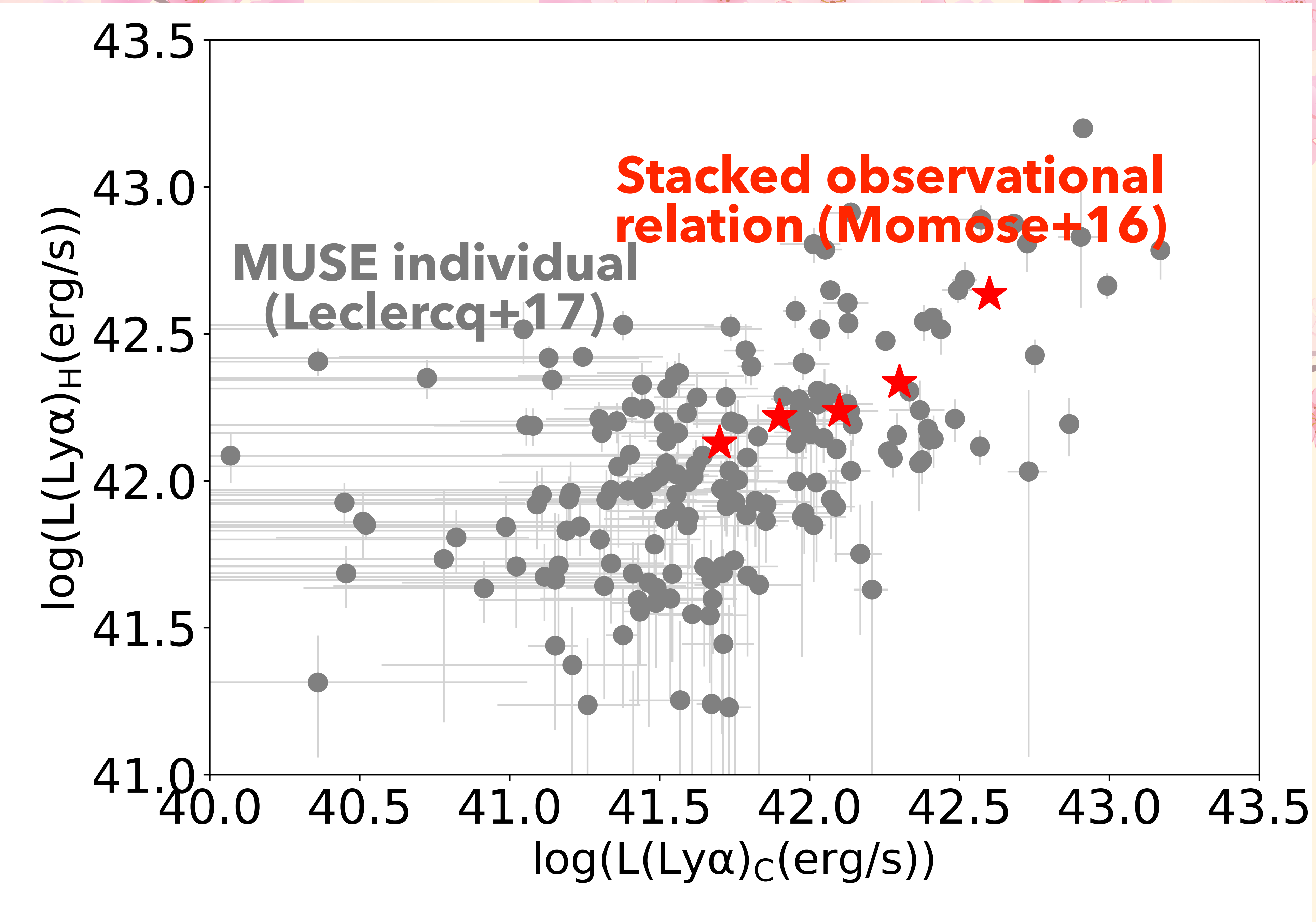

Estimating $L(Ly\alpha)_H$ from $L(Ly\alpha)_C$

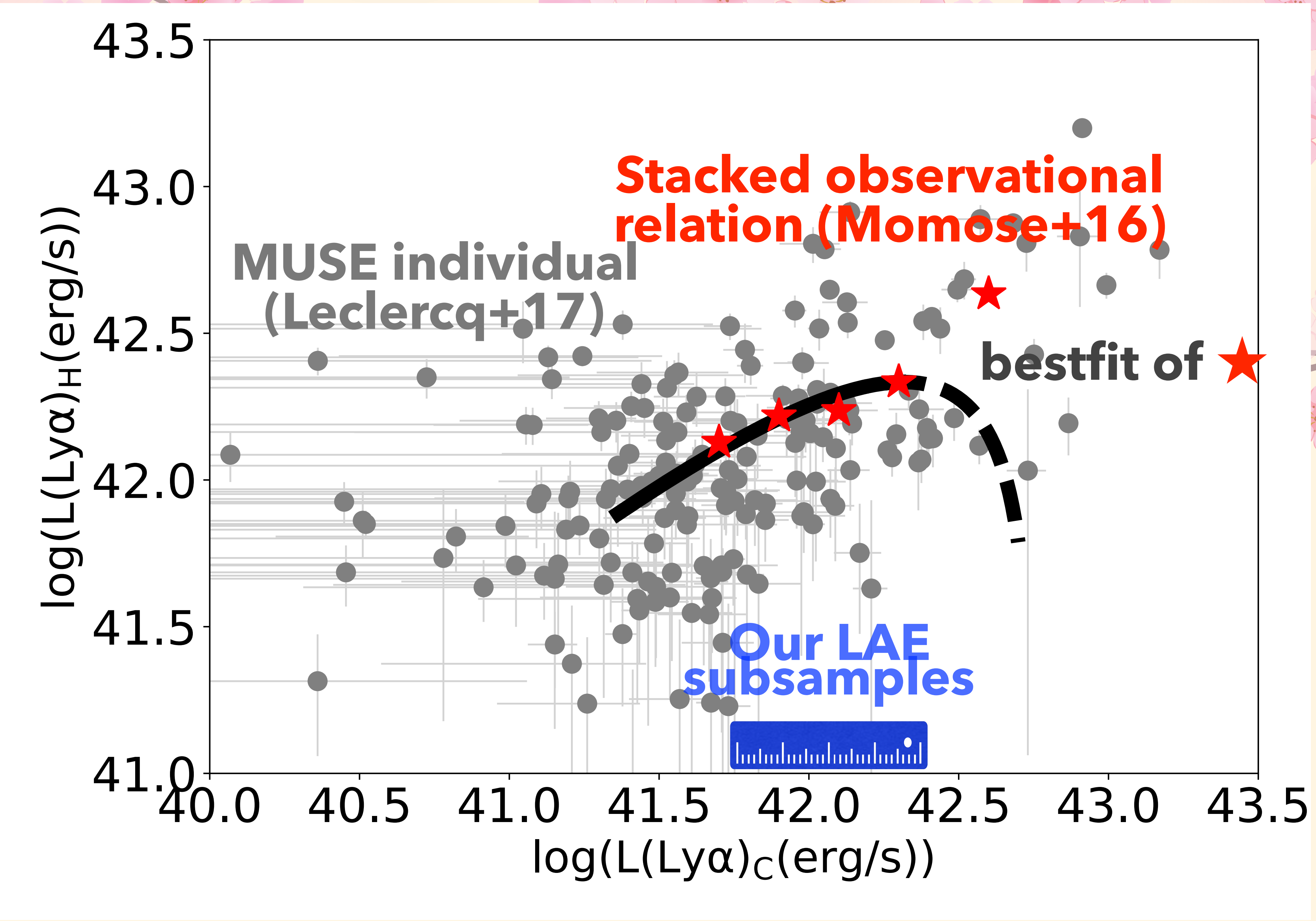

clustering analysis & SED fitting

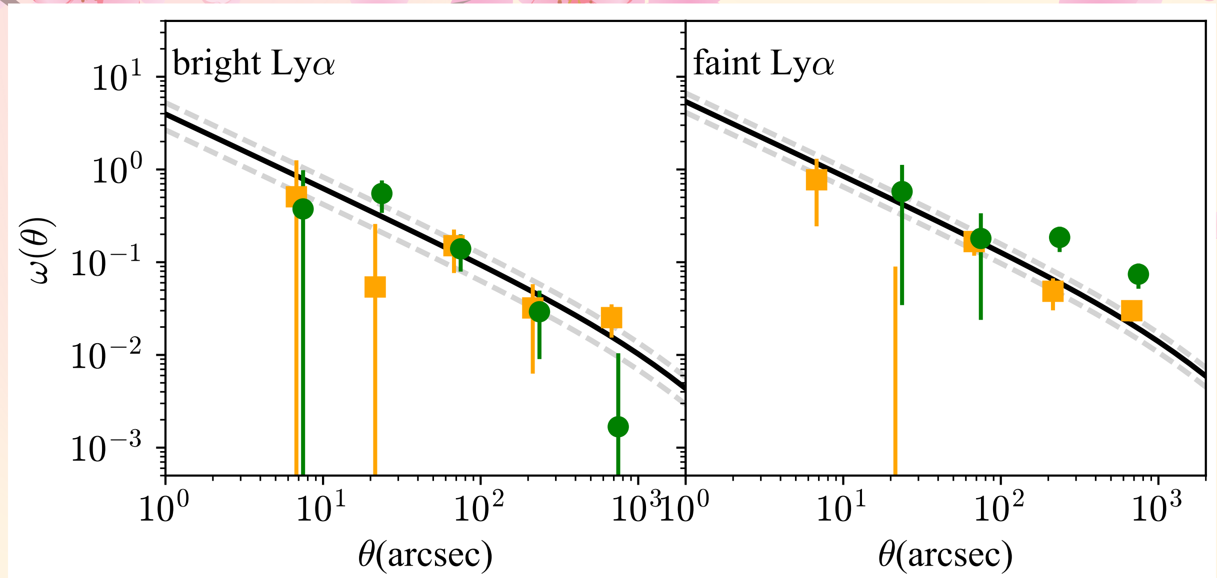

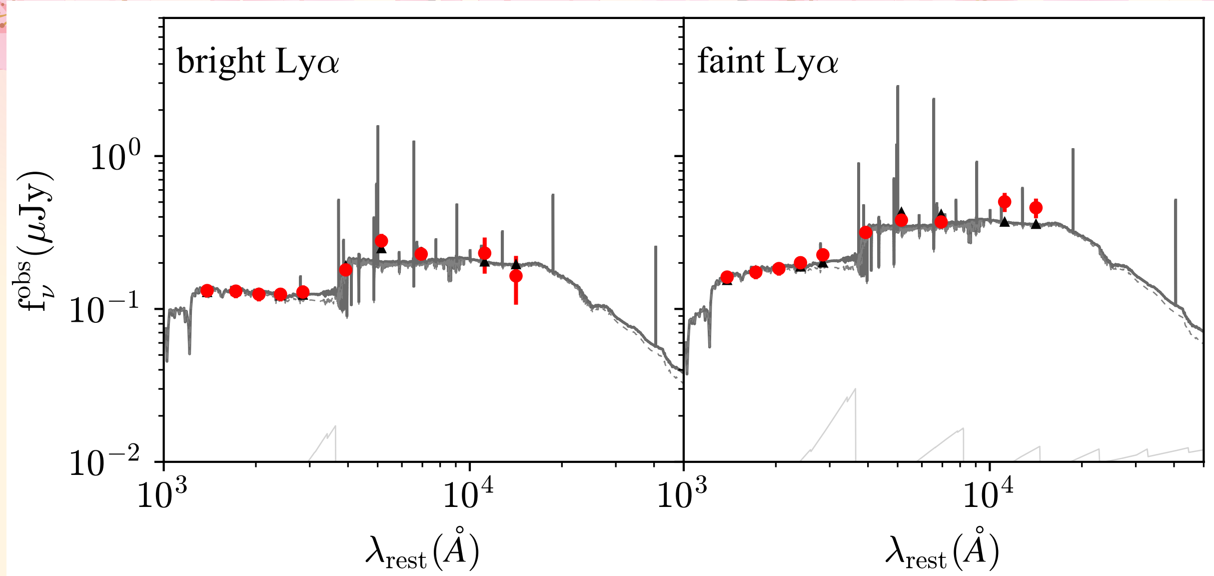

derived parameters: Mh

ACF: Landy & Szalay 1993
γ=1.8: Ouchi+2010
ro-Mh: Tinker+2010; Eisenstein & Hu 1998, 1999
fitting range=40-1000", Contami fraction=0-20%
: HK+2018a;

SFR, $M_\star$, age, E(B-V)

B, V, R, I, z, J, H, K, IRAC ch1 & ch2
SSP: Bruzual & Charlot 2003
nebula: Ono+2010
$E(B-V)_\star$ = E(B-V)g: Erb+2006
SMC-like curve: Gordon+2003; HK+2015
fesc(ion)=0.2: Nester+2013

with the same methods as in HK+2018a

Results and Discussion:

- The dominant origin of LAHs

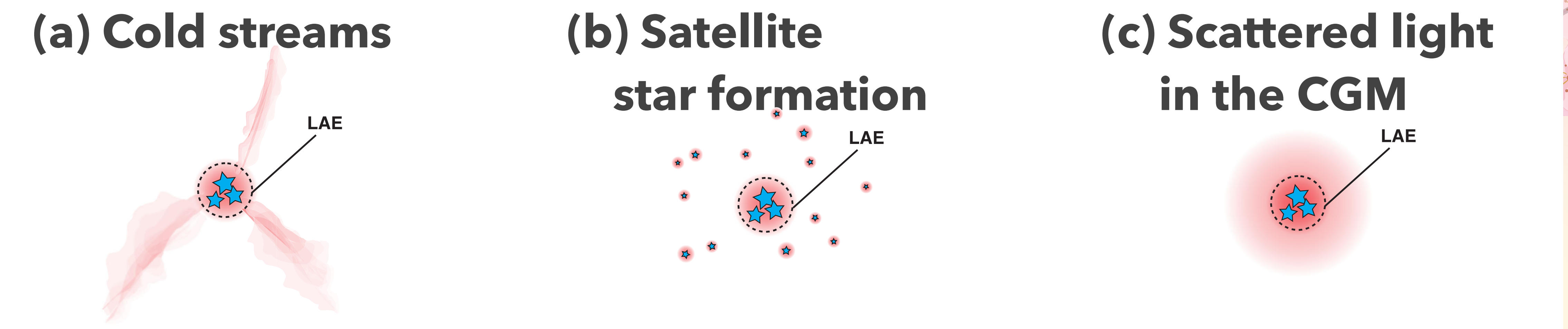

- Lyα escape fraction

L(Lya)$_H$ vs. Mass

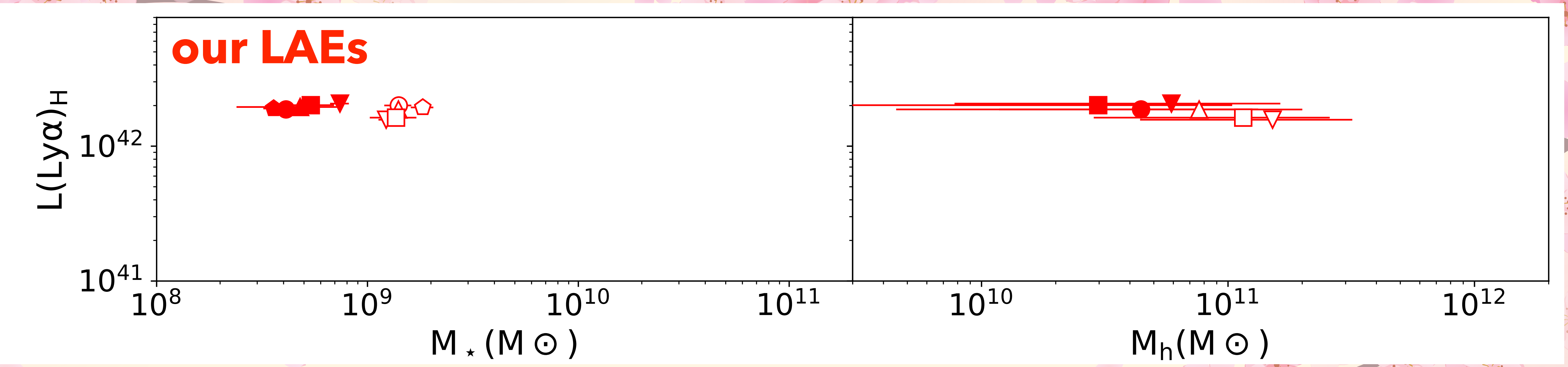

LAEs: nearly flat slope & high L(Lya)$_H$

Goerdt+2010; Rosdahl & Blaizot 2012; Moster+2013; Matthee+2016

(a) Cold streams (cooling radiation)

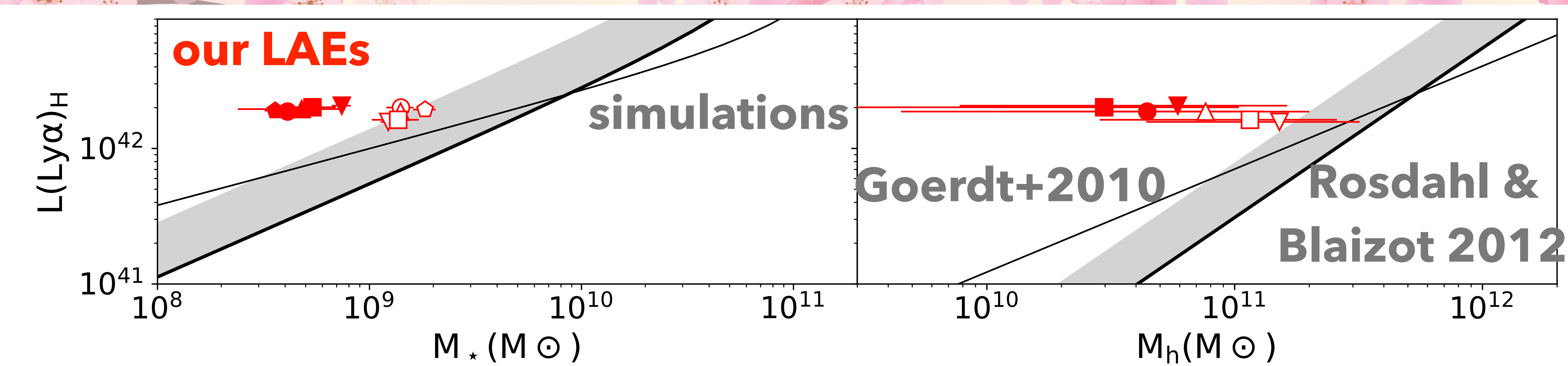

LAEs: nearly flat slope & high $L(Lya)_H$

Simulations: steeper slope ($\propto Mh^{0.8\text{-}1.3}$, >2σ)

lower $L(Lya)_H$ for low-$M_\star$ objects (>10σ)

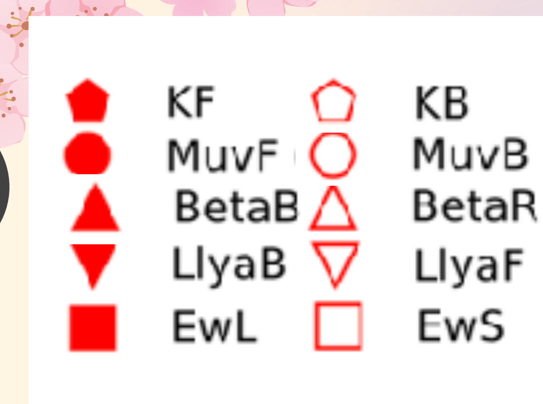

Note: Redshift correction of $L(Lya)_H \propto (1+z)^{1.3}$ applied (Goerdt+2010)

Mh→Ms with SHMR at z~2 in Moster+2013

(a) Cold streams (cooling radiation)

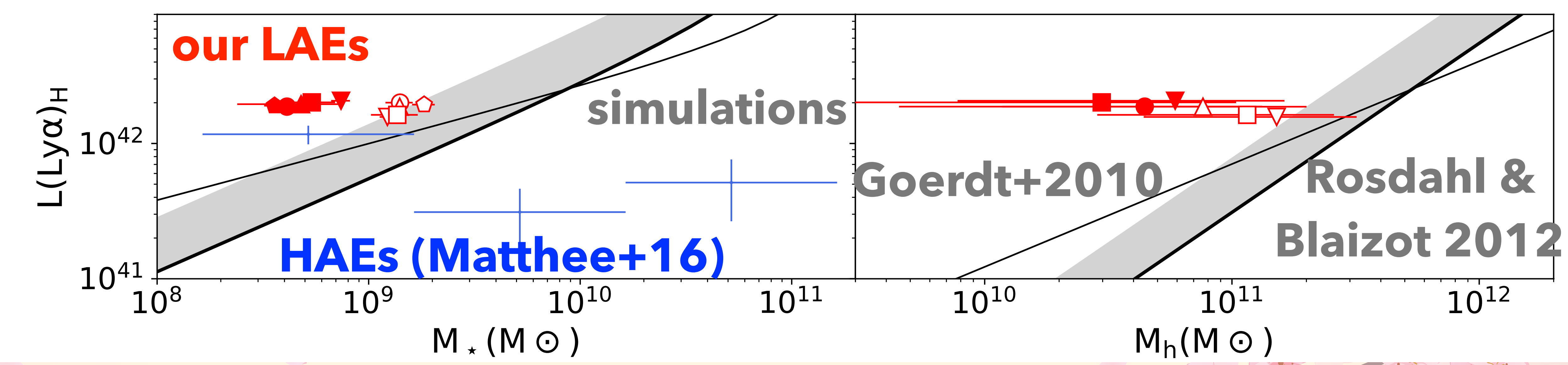

LAEs: nearly flat slope & high $L(Lya)_H$

Simulations: steeper slope ($\propto Mh^{0.8\text{-}1.3}$, >2σ)

lower $L(Lya)_H$ for low-$M_\star$ objects (>10σ)

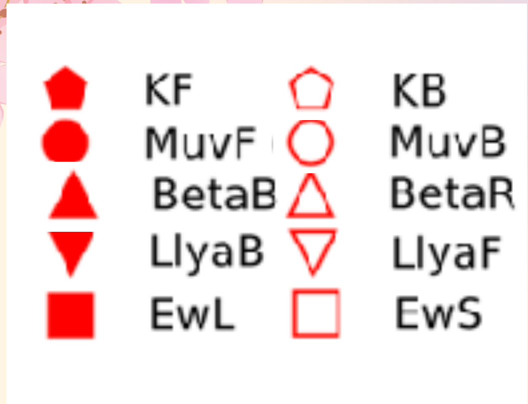

HAEs: nearly flat slope

→ not the dominant origin of LAHs

Note: Redshift correction of $L(Lya)_H \propto (1+z)^{1.3}$ applied in Goerdt+2010

Mh→Ms with SHMR at z~2 in Moster+2013

(b) Satellite star formation

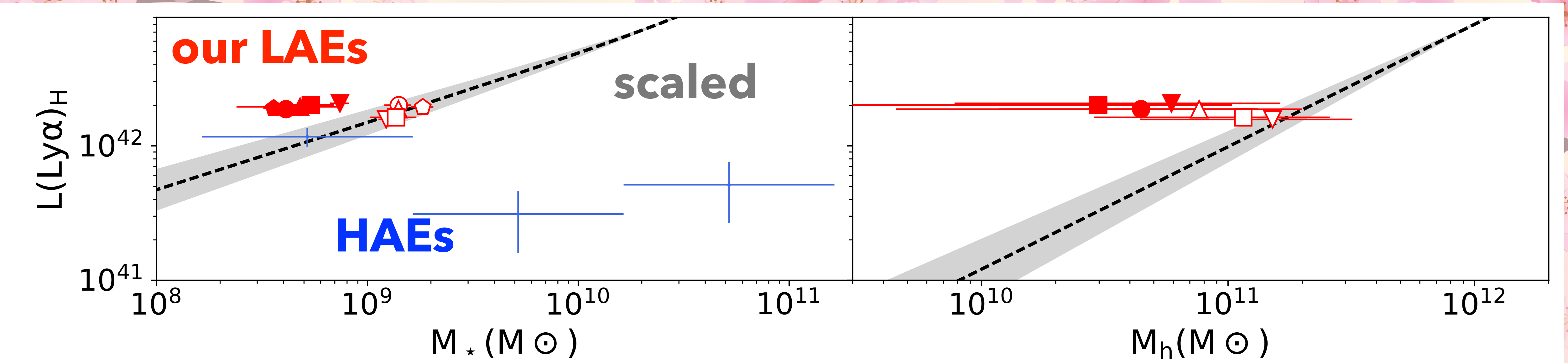

LAEs: nearly flat slope

HAEs: nearly flat slope

Obs. & Simu. : the number of satellites increases w the Mh ($\propto Mh^{0.91\pm0.11}$) and $M_\star$

→ not the dominant origin of LAHs

Note: arbitrary normalization

Trenthman & Tully 2009; Wang+2014; Tal+2013; Okamoto+2010; Moster+2013; Matthee+2016

(c) Scattered light in the CGM

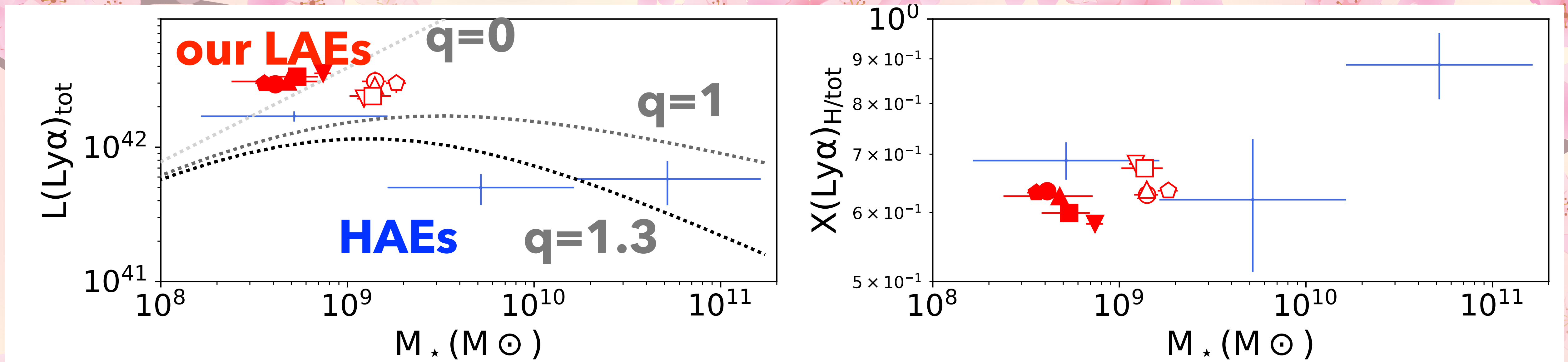

Model: L(Lya) H = L(Lya) tot * X(Lya)H/tot

Shivaei+2017; Heinis+2014; Matthee+2016

(c) Scattered light in the CGM

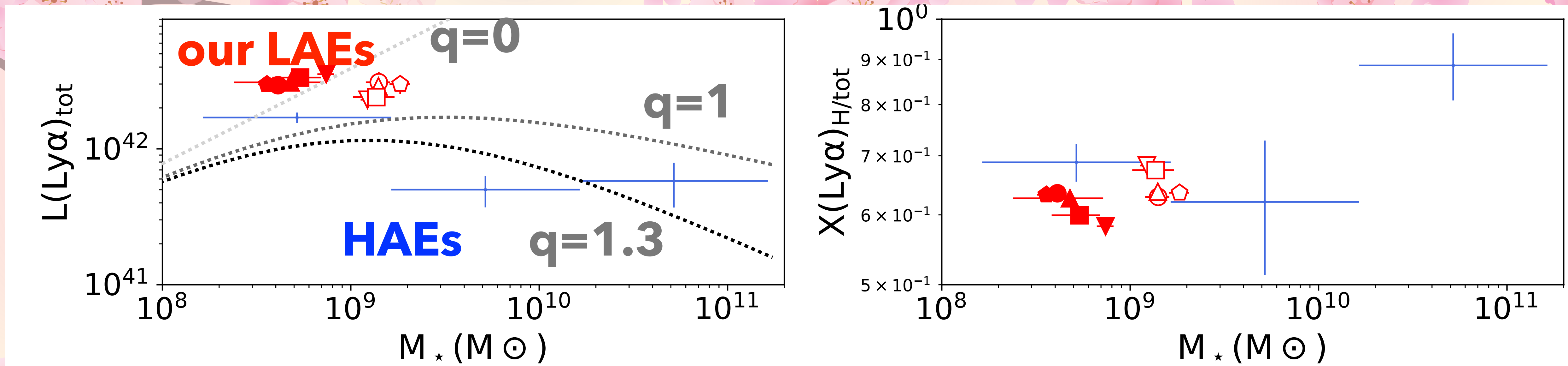

Model: $L(Ly\alpha)_H = L(Ly\alpha)_{tot} * X(Ly\alpha)_{H/tot}$

$L(Ly\alpha)_{tot} = L(Ly\alpha)_{SFR(M_\bigstar)} * 10\hat{}(-A_{1216\text{Å}con}(M_\bigstar)*q)$

$q = A_{Ly\alpha}/A_{1216\text{Å}con}(M_\bigstar)$

LAEs & HAEs: can be explained by varying q and X

→ the dominant origin of LAHs

Shivaei+2017; Heinis+2014; Matthee+2016

High Lyα escape fraction (C+H)

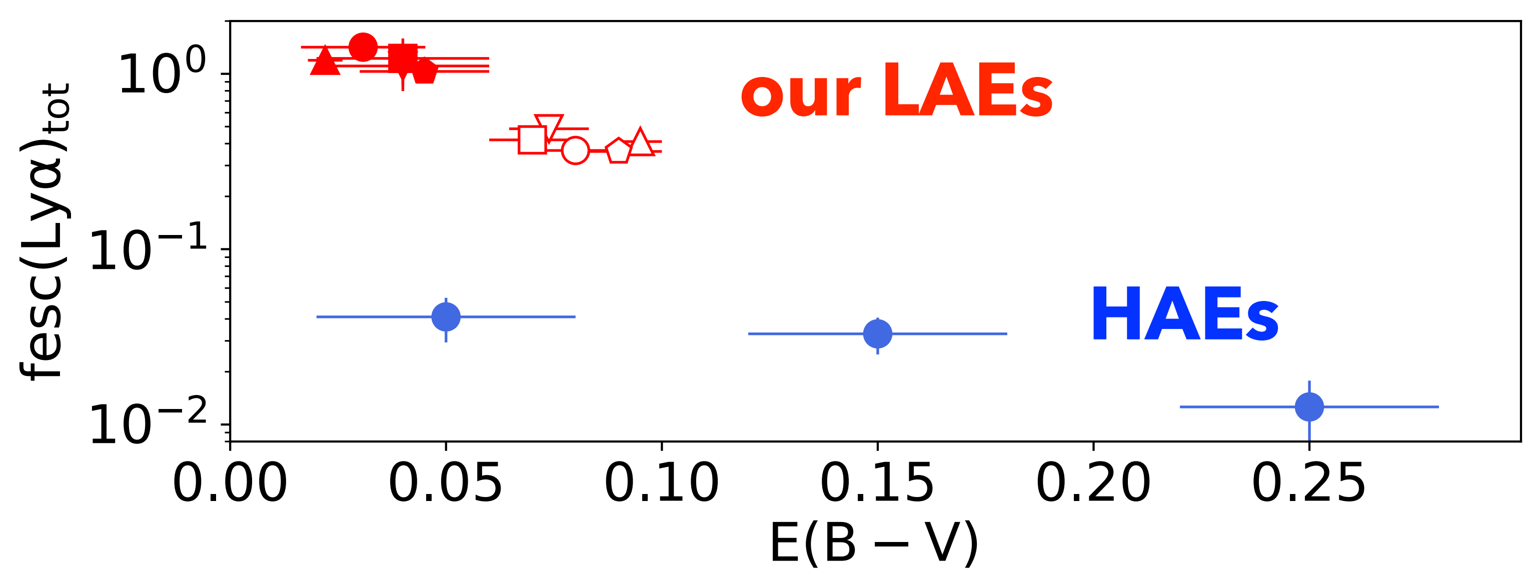

$$f_{\rm esc}({\rm Ly}\alpha)_{\rm tot} = \frac{L({\rm Ly}\alpha)_C + L({\rm Ly}\alpha)_H}{L({\rm Ly}\alpha)_{SFR}}$$

Anti-correlation of fesc(Lya) - E(B-V), SFR, & $M_\star$

1dex higher than HAEs with similar E(B-V) and $M_\star$

very high fesc (Lya) >~100%

- **low HI gas mass (low Mh)**
- **hard ionizing spectrum than expected**

Matthee+2016; Cochrane+2018; Nakajima+18

Summary

LAH vs $M_\star$ & Mh for ~900 NB-selected LAEs at z~2

- stacked $L(Ly\alpha)_C$-$L(Ly\alpha)_H$ relation is consistent with the MUSE results

Dominant origin of LAHs

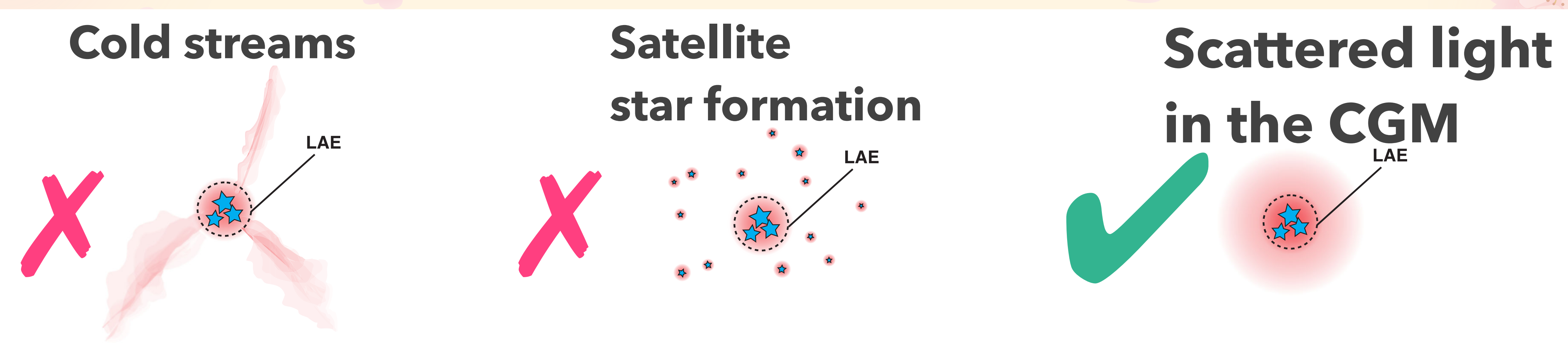

LAEs have a higher fesc(Lya) than HAEs with similar E(B-V)

- Low HI gas mass and/or hard ionizing spectrum

- Hα spectroscopic observation will give further information!
- HSC (CHORUS & SILVERRUSH) enables us to derive Mh accurately!

Appendix

Table 2. Subsample definition.

subsample	criteria	COSMOS	SXDS	total
bright UV (MuvB)	$M_{UV} \leq -19.2\,\mathrm{mag}$	123 (123, 9)	293 (257, 52)	416 (380, 61)
faint UV (MuvF)	$M_{UV} > -19.2\,\mathrm{mag}$	173 (173, 13)	302 (257, 47)	475 (430, 60)
blue β (betaB)	$\beta \leq -1.6$	80 (80, 5)	389 (334, 74)	469 (414, 79)
red β (betaR)	$\beta > -1.6$	216 (216, 17)	206 (180, 25)	422 (396, 42)
bright Lyα (lyaB)	$L(\mathrm{Ly}\alpha)_{ps} \geq 1.2 \times 10^{42}\,\mathrm{erg\,s^{-1}}$	211 (211, 14)	236 (218, 41)	447 (429, 55)
faint Lyα (lyaB)	$L(\mathrm{Ly}\alpha)_{ps} < 1.2 \times 10^{42}\,\mathrm{erg\,s^{-1}}$	85 (85, 8)	359 (296, 58)	444 (381, 66)
large EW (ewL)	$EW_{0,\,ps}(\mathrm{Ly}\alpha) \geq 34\,\mathrm{Å}$	222 (222, 16)	228 (205, 35)	450 (427, 51)
small EW (ewS)	$EW_{0,\,ps}(\mathrm{Ly}\alpha) < 34\,\mathrm{Å}$	74 (74, 6)	367 (309, 64)	441 (383, 70)
bright K (KB)	$m_{\mathrm{K}} \leq 25\,\mathrm{mag}$	112 (112, 11)	178 (177, 35)	290 (144, 46)
faint K (KF)	$m_{\mathrm{K}} > 25\,\mathrm{mag}$	184 (184, 11)	417 (337, 64)	601 (236, 75)

Note. The selection criterion and the numbers of objects for each subsample. The number outside the bracket indicates the number of objects for clustering analysis, while the numbers in the bracket are for SED fitting: the left one corresponds to objects with UV to NIR photometry and the right one to those with clean ch1 and ch2 photometry.

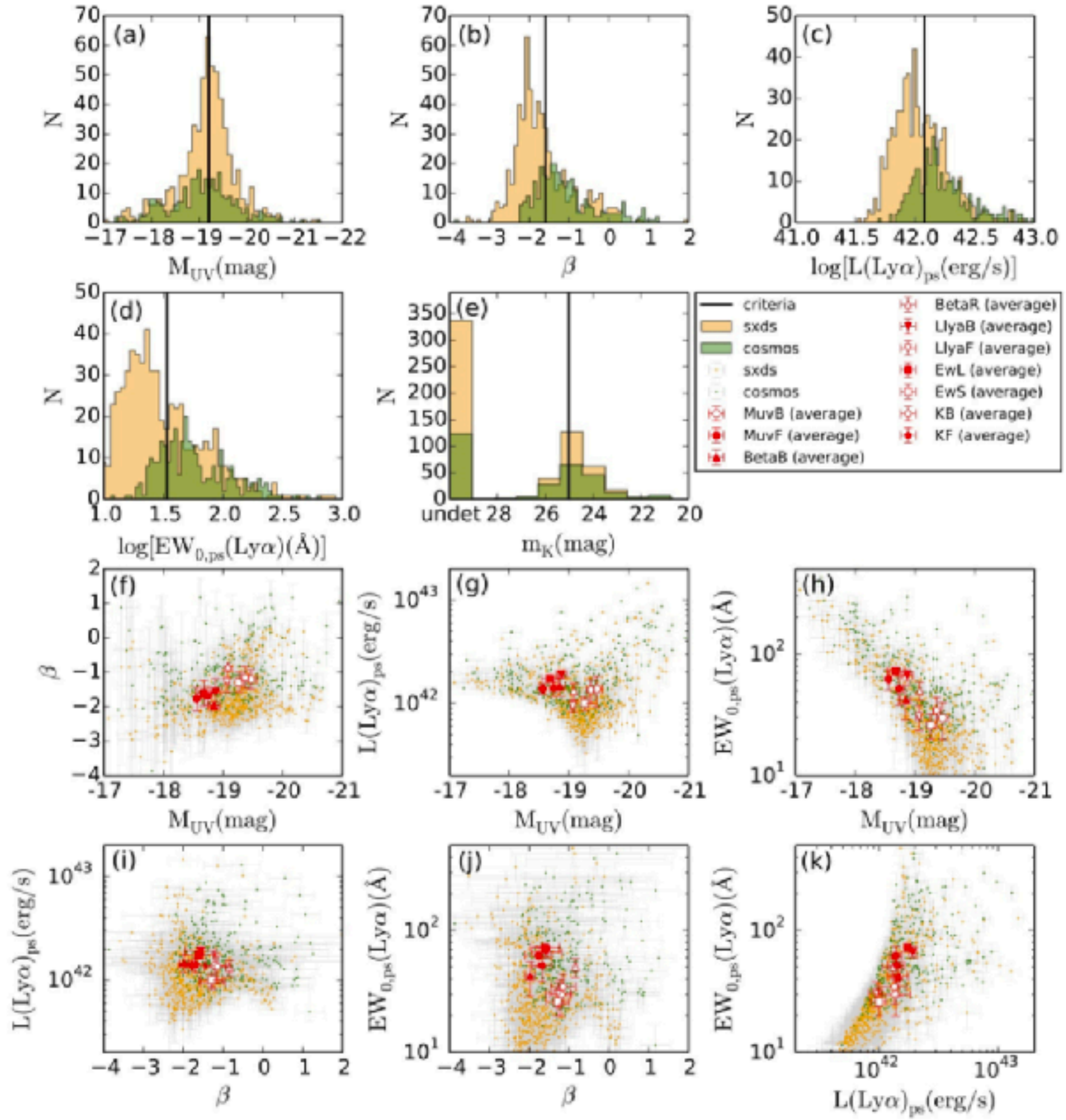

Fig. 1. The distribution of the five quantities used to divide our LAEs into subsamples. Panels (a) – (e) show histograms: (a) $M_{\rm UV}$, (b) β, (c) $L(\rm Ly\alpha)_{ps}$, (d) $EW_{0,ps}(\rm Ly\alpha)$, and (e) $m_{\rm K}$, with orange and green colors corresponding to the SXDS and COSMOS fields, respectively. Black lines indicate the boundaries of the two subsamples. Panels (f) – (k) are scatter plots: (f) $M_{\rm UV}$ vs. β, (g) $M_{\rm UV}$ vs. $L(\rm Ly\alpha)_{ps}$, (h) $M_{\rm UV}$ vs. $EW_{0,ps}(\rm Ly\alpha)$, (i) β vs. $L(\rm Ly\alpha)_{ps}$, (j) β vs. $EW_{0,ps}(\rm Ly\alpha)$, and (k) $L(\rm Ly\alpha)_{ps}$ vs. $EW_{0,ps}(\rm Ly\alpha)$, with the same color coding as panels (a)–(d). Red symbols represent averages over the two fields, where different symbols correspond to different classifications: open (filled) circles for bright (faint) $M_{\rm UV}$, open (filled) triangles for red (blue) β, open (filled) inverted triangles for faint (bright) $L(\rm Ly\alpha)_{ps}$, open (filled) squares for large (small) EW, and open (filled) pentagons for bright (faint) $m_{\rm K}$.

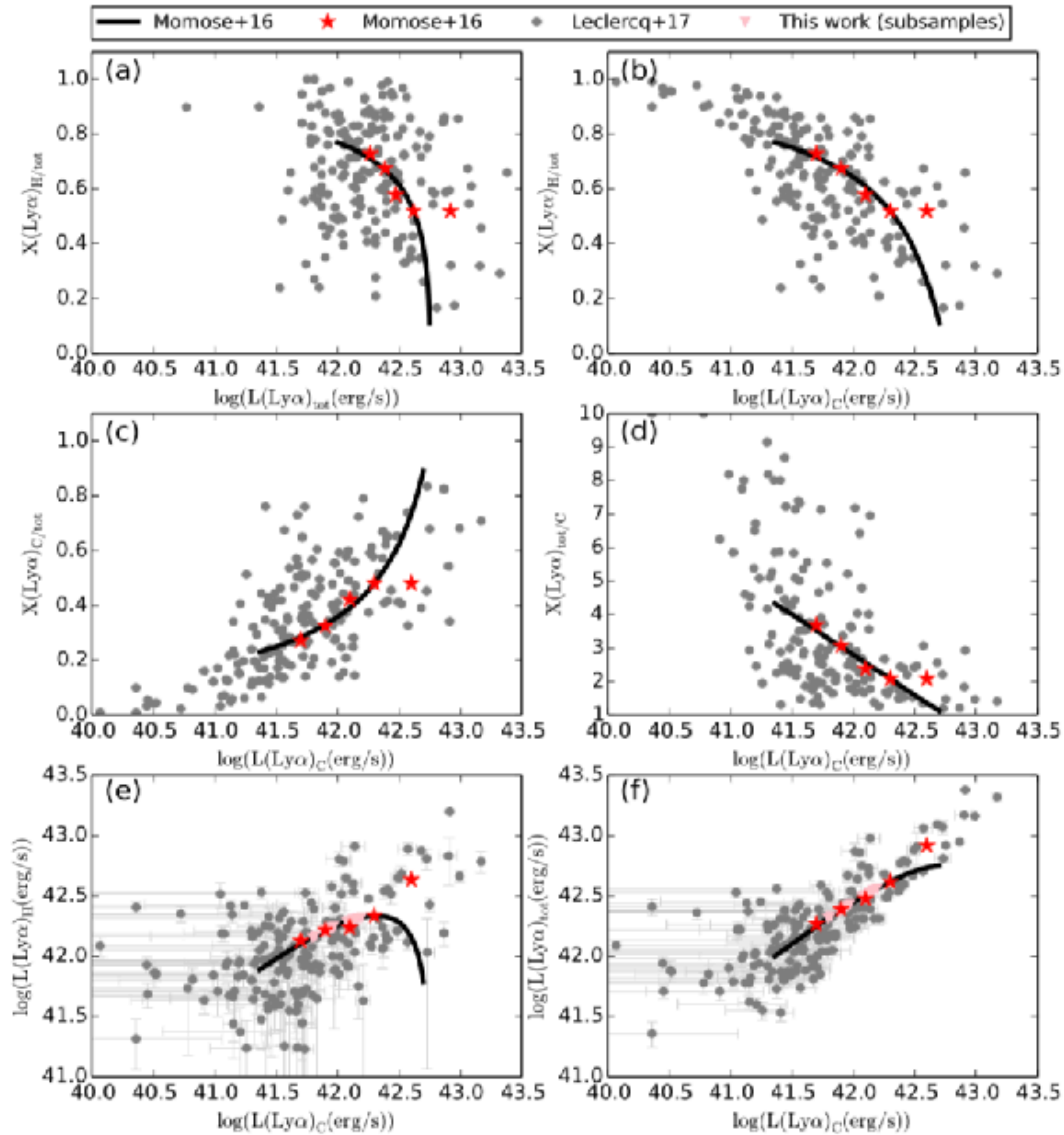

Fig. 2. Relation between $L\mathrm{Ly}\alpha)_H$ and $L\mathrm{Ly}\alpha)_C$ in six different presentations. (a) $L\mathrm{Ly}\alpha)_H/L\mathrm{Ly}\alpha)_{tot}$ vs. $L\mathrm{Ly}\alpha)_{tot}$; (b) $L\mathrm{Ly}\alpha)_H/L\mathrm{Ly}\alpha)_{tot}$ vs. $L\mathrm{Ly}\alpha)_C$; (c) $L\mathrm{Ly}\alpha)_C/L\mathrm{Ly}\alpha)_{tot}$ vs. $L\mathrm{Ly}\alpha)_C$; (d) $L\mathrm{Ly}\alpha)_{tot}/L\mathrm{Ly}\alpha)_C$ vs. $L\mathrm{Ly}\alpha)_C$; (e) $L\mathrm{Ly}\alpha)_H$ vs. $L\mathrm{Ly}\alpha)_C$; and (f) $L\mathrm{Ly}\alpha)_{tot}$ vs $L\mathrm{Ly}\alpha)_C$. Red stars and black lines indicate, respectively, the stacked results and their best-fit relation given by Momose et al. (2016). The best-fit linear relation is determined in panel (d) and is shown in equation 10. Grey points represents MUSE-LAEs at $z \sim 3-6$ Leclercq et al. (2017), where error are only shown in panels (e) and (f). Pink inverted triangles in panels (e) and (f) show the $L\mathrm{Ly}\alpha)_H$ and $L\mathrm{Ly}\alpha)_{tot}$ of our subsamples calculated from $L\mathrm{Ly}\alpha)_C$ using the empirical relation in Momose et al. (2016). (Color online)

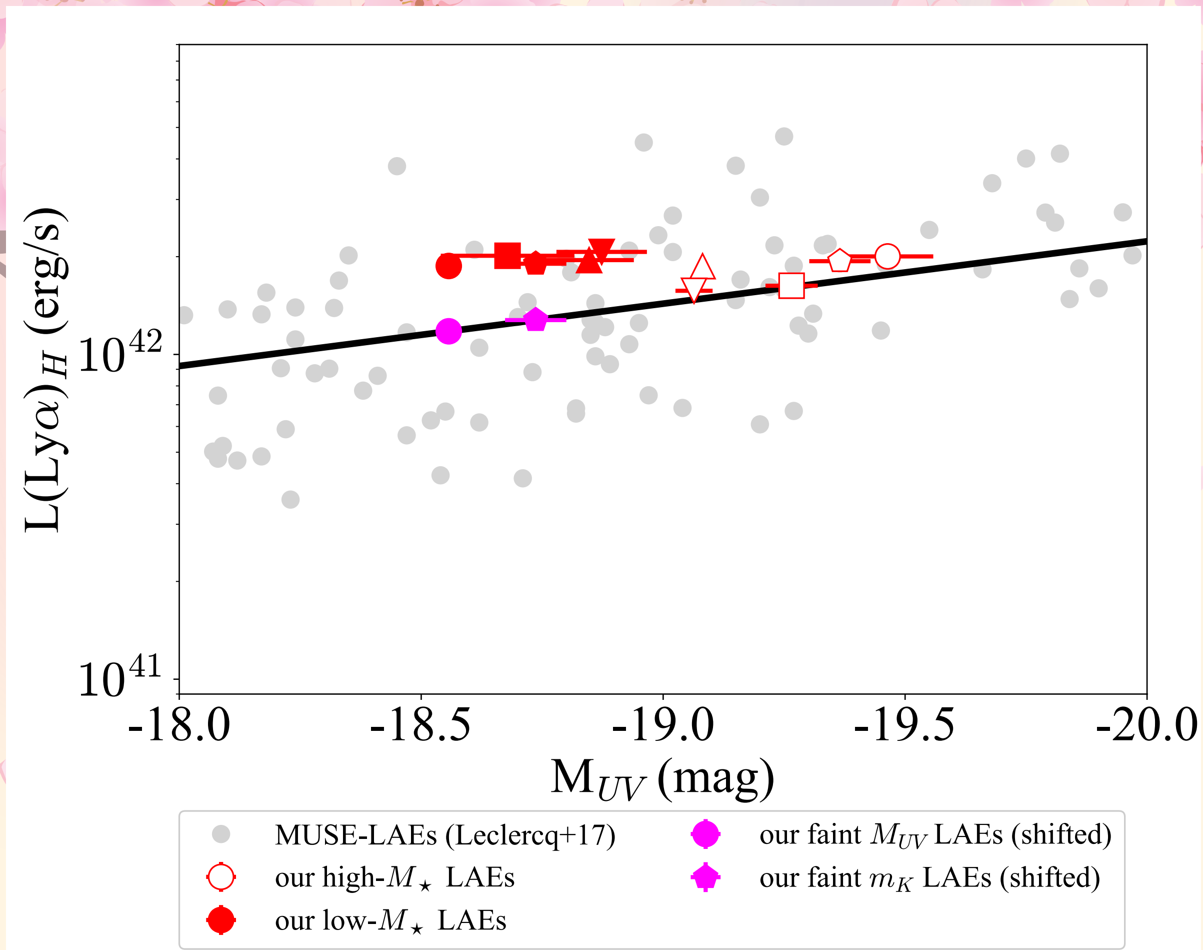

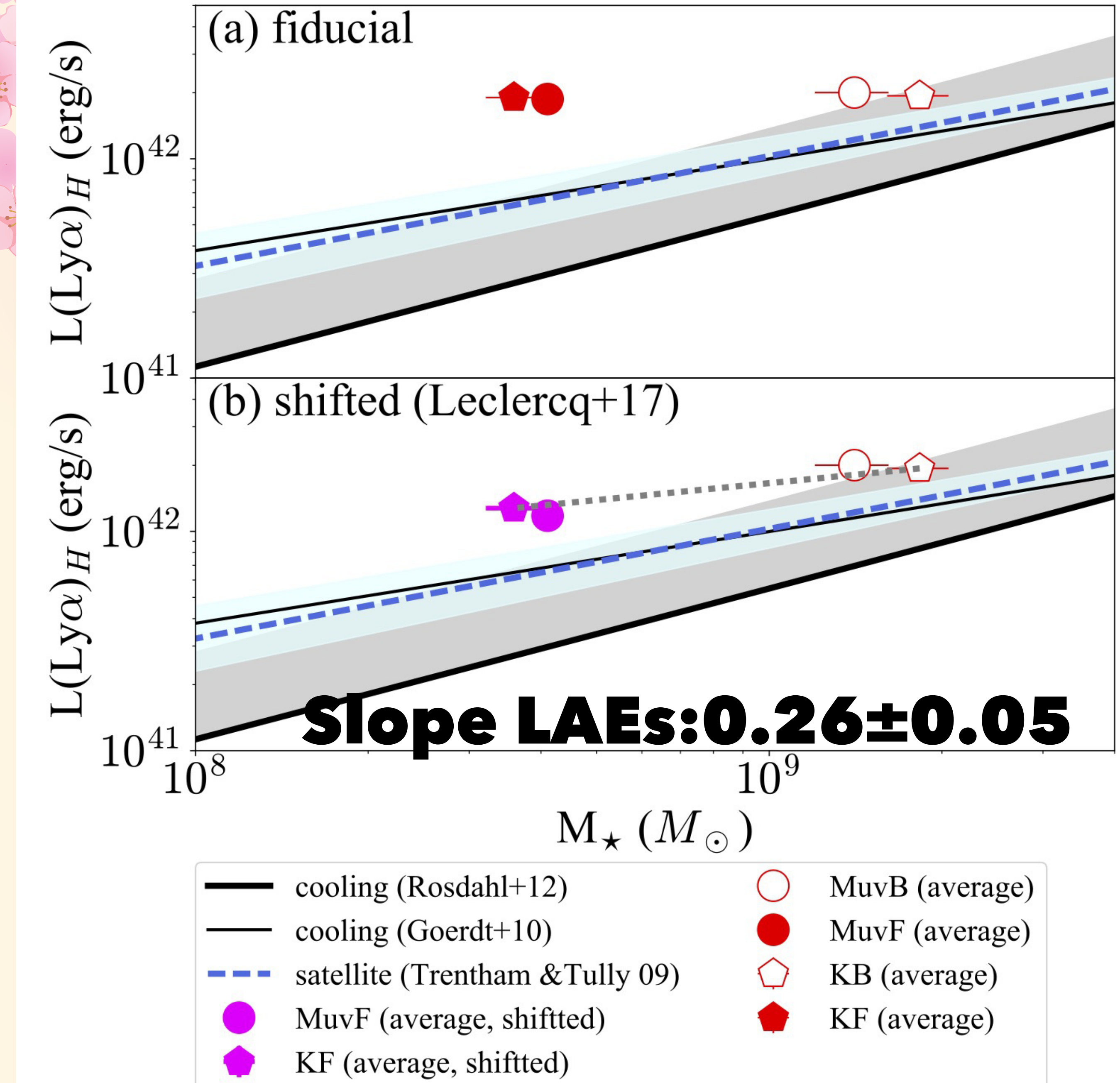

Cold stream:~0.38, 0.75,

Satellite SF:~0.40±0.13

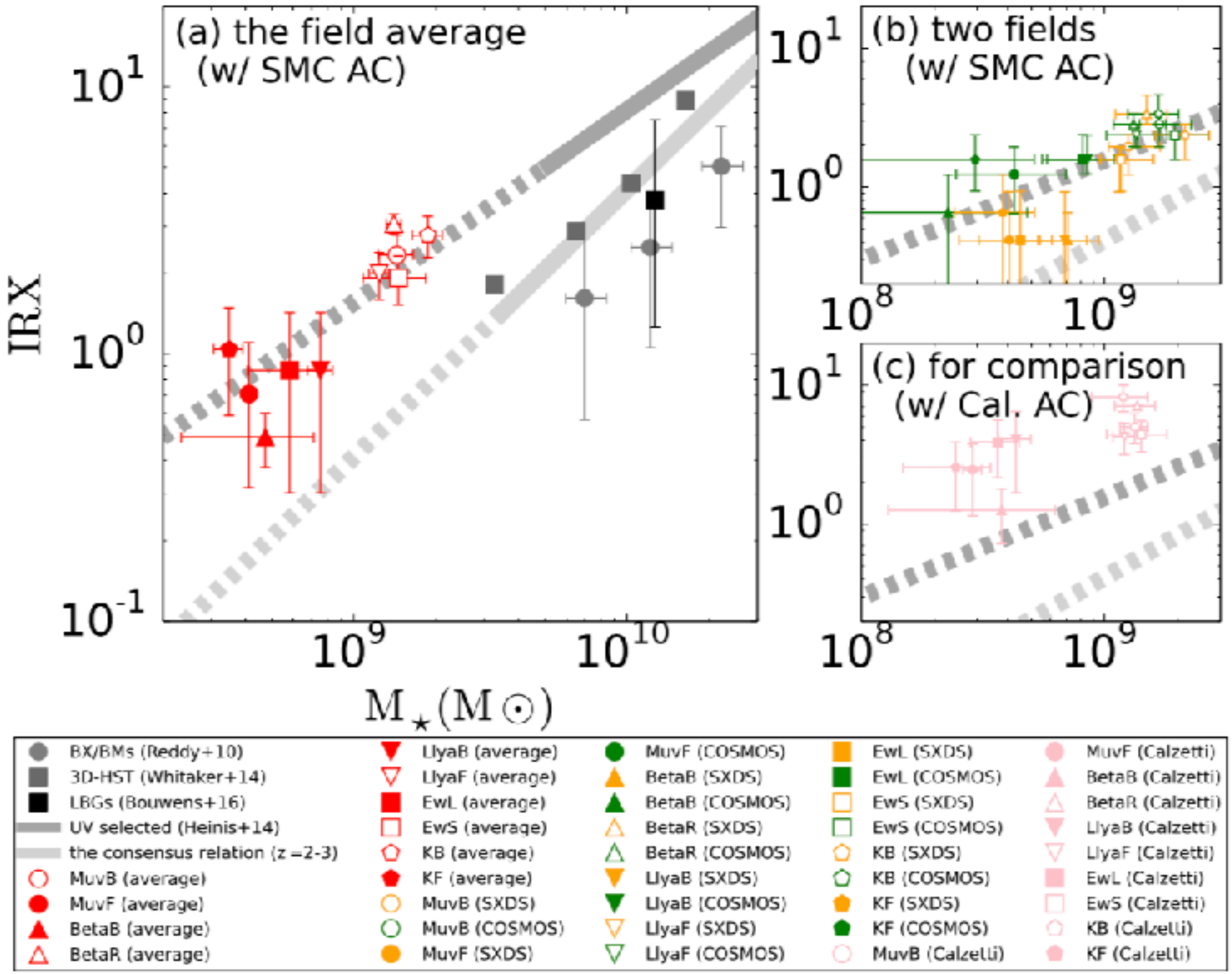

Fig. 3. IRX vs $M_\star$. (a) Field average values of our ten subsamples with an assumption of a SMC-like attenuation curve (red symbols), (b) results before averaging (green and yellow symbols),and (c) field average values with an assumption of a Calzetti curve (pink symbols), plotted with some literature results. In panels (a) and (c), different subsamples are shown by different symbols: open (filled) circles for bright (faint) $M_{\rm UV}$, open (filled) triangles for red (blue) β, open (filled) inverted triangles for faint (bright) $L({\rm Ly}\alpha)_{\rm ps}$, open (filled) squares for small (large) $EW_{0,\rm ps}({\rm Ly}\alpha)$, and open (filled) pentagons for bright (faint) m_K. Dark gray squares, dark gray circles, a black square, a dark gray solid line and a light gray solid line represent, respectively, 3D-HST galaxies at $z \sim 2$ in Whitaker et al. (2014), UV selected galaxies at $z \sim 2$ in Reddy et al. (2010), LBGs at $z \sim 2-3$ in Bouwens et al. (2016), UV-selected galaxies at $z \sim 1.5$ in Heinis et al. (2014) and the consensus relation of them determined by Bouwens et al. (2016). Dark and light gray dashed lines indicate extrapolations of gray solid lines. All data are rescaled to a Salpeter IMF according to footnote 1. (Color online)

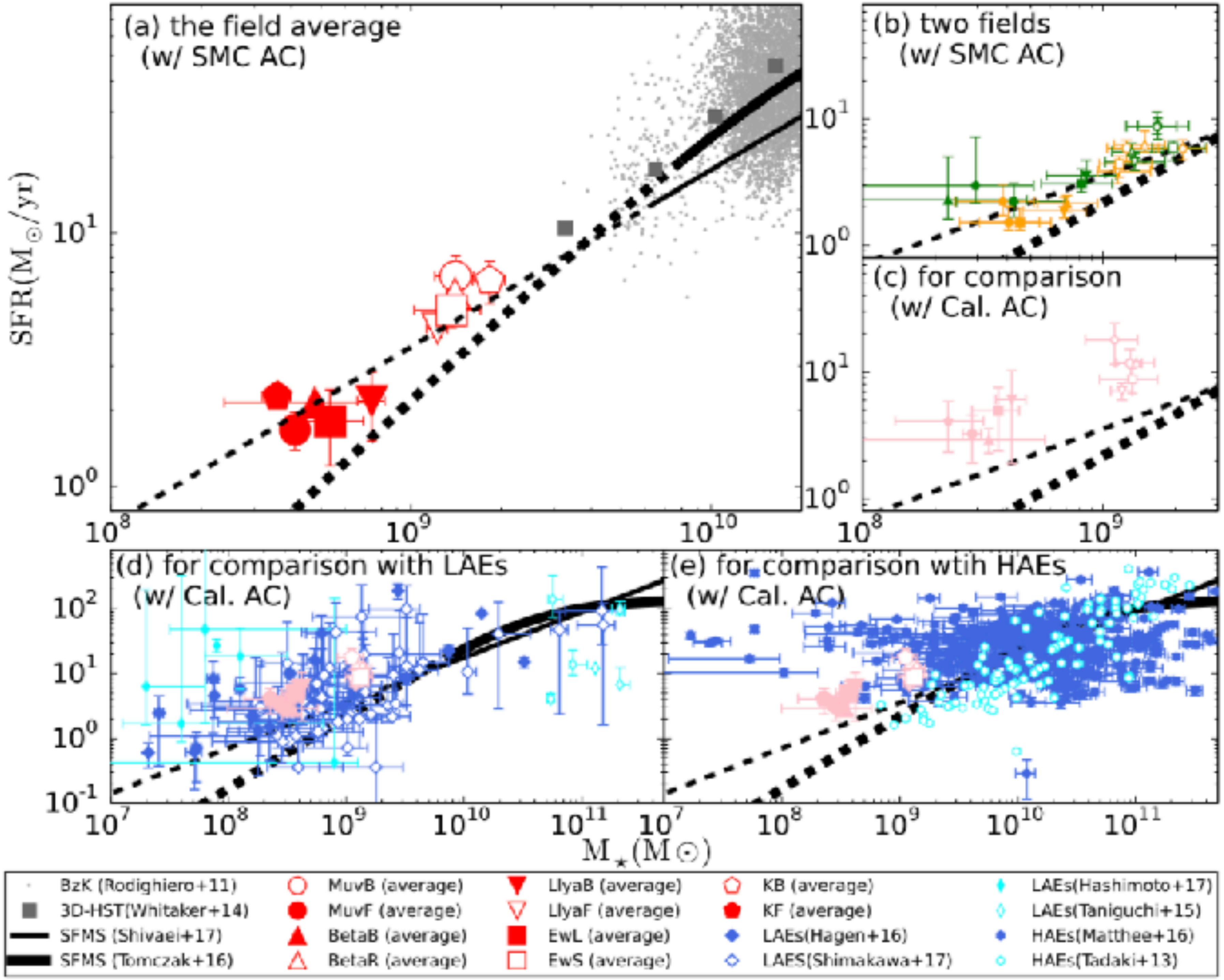

Fig. 4. SFR vs $M_{\star}$. (a) Field average values of our ten subsamples with a SMC-like attenuation curve (red symbols), (b) results before averaging (green and yellow symbols), and (c)-(e) field average values with a Calzetti curve (pink symbols), plotted with some literature results. In panels (a) and (c)–(e), different subsamples are shown by different symbols: open (filled) circles for bright (faint) $M_{\rm UV}$, open (filled) triangles for red (blue) β, open (filled) inverted triangles for faint (bright) $L({\rm Ly}\alpha)_{ps}$, open (filled) squares for small (large) $EW_{0,ps}({\rm Ly}\alpha)$, and open (filled) pentagons for bright (faint) $m_{\rm K}$. In panel (b), orange and green symbols indicate, respectively, the SXDS and COSMOS subsamples with a SMC-like attenuation curve (w/ SMC AC). In panels (c)–(e), pink symbols show the average values of the subsamples over the two fields with a Calzetti attenuation curve (W/ Cal AC). Dark gray squares, light gray dots, thick black solid lines, and thin black solid lines represent, respectively, 3D-HST galaxies at $z \sim 2$ in Whitaker et al. (2014), BzK galaxies at $z \sim 2$ in Rodighiero et al. (2011), the SFMS at $z \sim 2$ in Tomczak et al. (2016), and the SFMS at $z \sim 2$ in Shivaei et al. (2017). Thick and thin black dashed lines indicate extrapolations of the black solid lines. In panel (d), filled blue diamonds, open blue diamonds, filled cyan thin diamonds, and open cyan thin diamonds indicate LAEs at $z \sim 2$–3 in Hagen et al. (2016); Shimakawa et al. (2017); Hashimoto et al. (2017) and Taniguchi et al. (2015), respectively. In panel (e), filled blue hexagons and open cyan hexagons show HAEs at $z \sim 2$–3 in Matthee et al. (2016) and Tadaki et al. (2013). All data are rescaled to a Salpeter IMF according to footnote 1. (Color online)

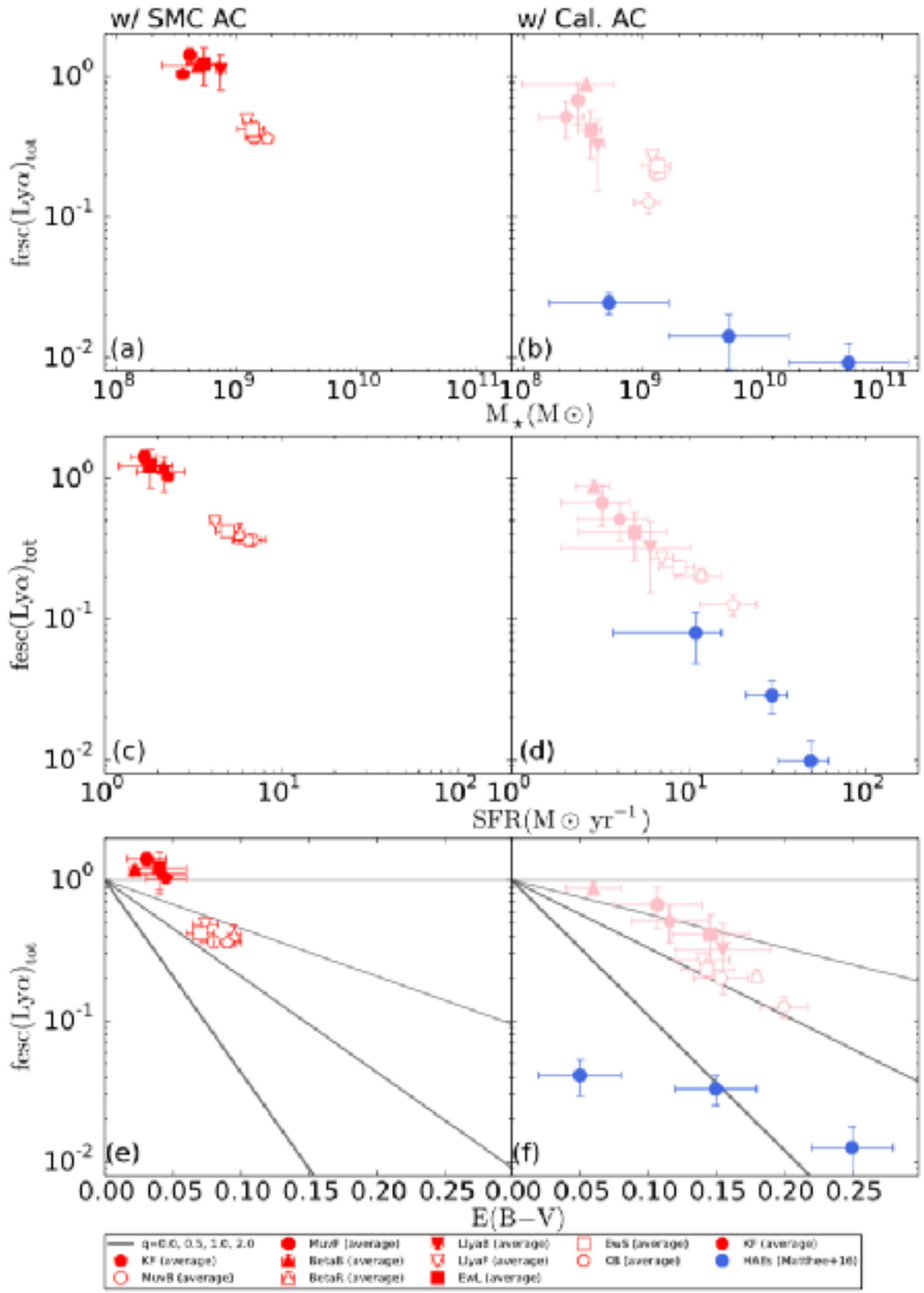

Fig. 6. $fesc(\mathrm{Ly}\alpha)_{tot}$ as a functions of M_* (panels [a] and [b]), SFR ([c] and [d]), and $E(B-V)$ ([e] and [f]) for the two attenuation curves. All values are field average values. Different symbols indicate different subsamples: open (filled) circles for bright (faint) M_{UV}, open (filled) triangles for red (blue) β, open (filled) inverted triangles for faint (bright) $L(\mathrm{Ly}\alpha)_{ps}$, open (filled) squares for small (large) $EW_{0,ps}(\mathrm{Ly}\alpha)$, and open (filled) pentagons for bright (faint) m_K. Filled blue circles indicate HAEs in Matthee et al. (2016), whose Lyα luminosities are derived from 6′′ aperture photometry. dark gray solid lines show models for four different q values, $q = 0.0, 0.5, 1.0$, and 2.0 with increasing thickness. Stellar parameters are derived with the assumptions of $E(B-V)_* = E(B-V)_g$ and $f_{esc}^{ion} = 0.2$. (Color online)

clustering analysis & SED fitting

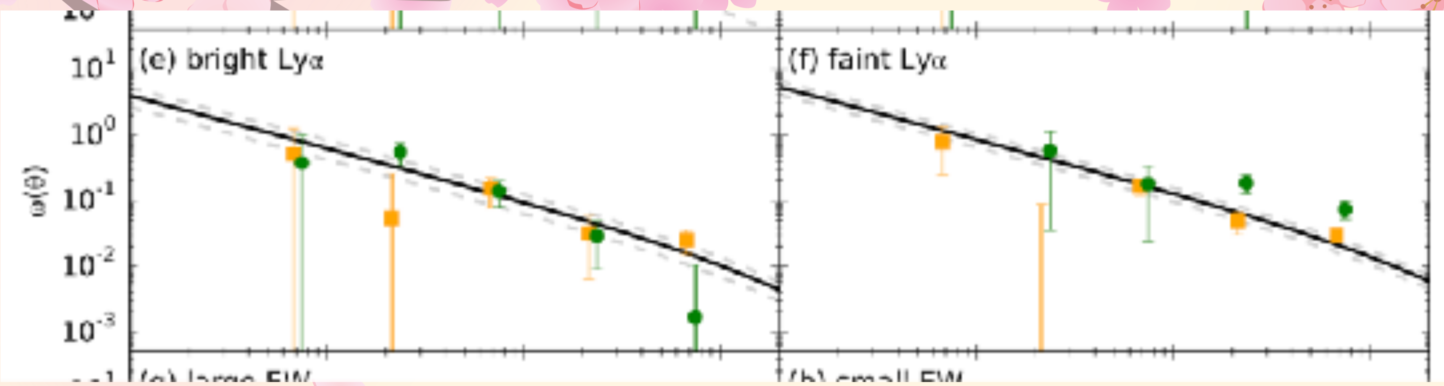

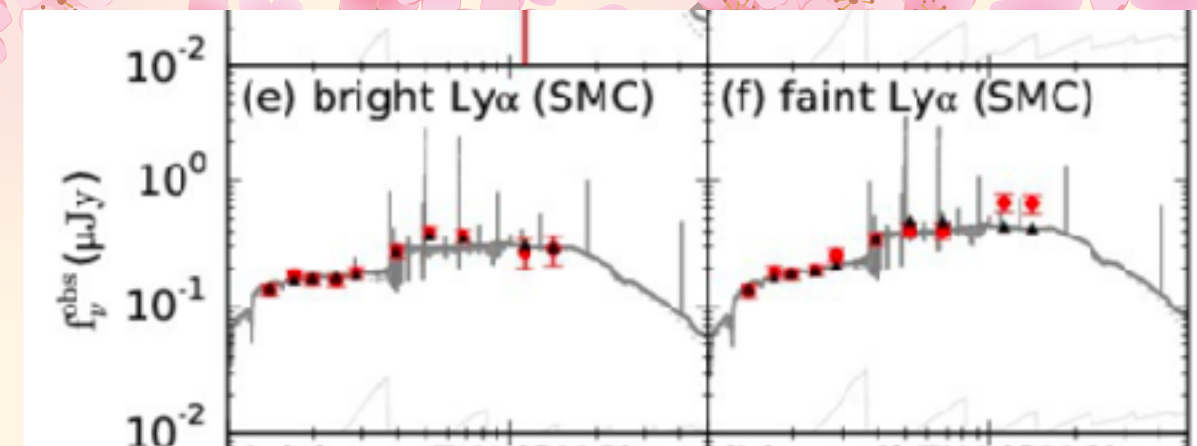

derived parameters: Mh

ACF: Landy & Szalay 1993
γ=1.8: Ouchi+2010
ro-Mh: Tinker+2010; Eisenstein & Hu 1998, 1999
fitting range=40-1000", Contami fraction=0-20%
: Kusakabe+2018a;

SFR, $M_\star$, age, E(B-V)

B, V, R, I, z, J, H, K, IRAC ch1 & ch2
SSP: Bruzual & Charlot 2003
nebula: Ono+2010
E(B-V)★ = E(B-V)g: Erb+2006
SMC-like curve: Gordon+2003; Kusakabe+2015
fesc(ion)=0.2: Nester+2013
the same as those in Kusakabe+2018a

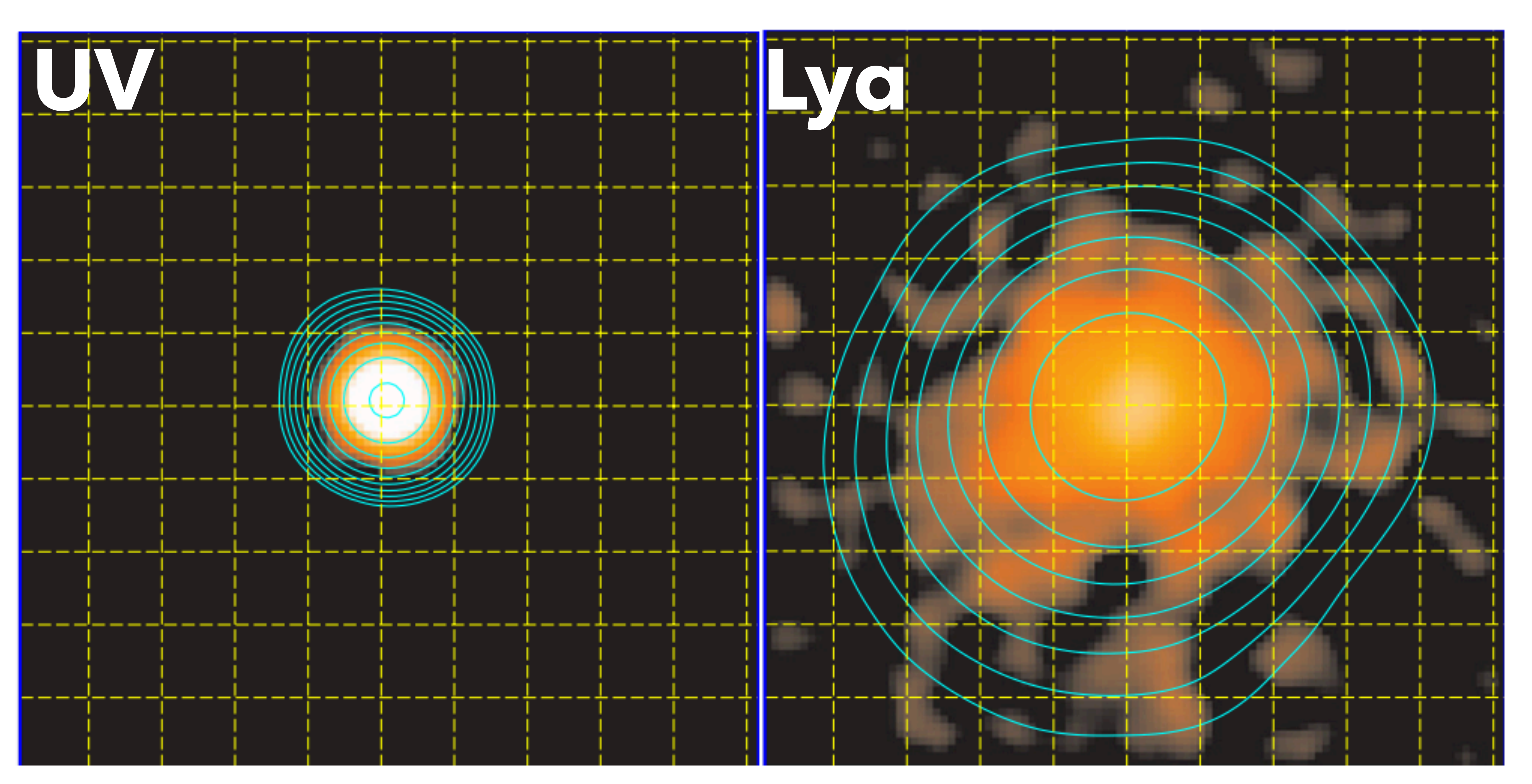

Steidel+2011

Spatially extended Lya emission

Lya halos (LAHs)